1992

Development of a Computer Simulation Program for the Acoustic Tuning of Rolling Piston Compressors

G. Prater
University of Louisville

E. E. Ratterman
Exxon Company USA

DEVELOPMENT OF A COMPUTER SIMULATION PROGRAM FOR THE ACOUSTIC TUNING OF ROLLING PISTON COMPRESSORS

Glen Prater, Jr., Assistant Professor
Department of Mechanical Engineering
University of Louisville
Louisville, KY 40292

Eugene E. Ratterman, Project Engineer
Exxon Company USA
1555 Poydras Street
New Orleans, LA 70012

ABSTRACT

A vapor compressor's performance is affected by pressure and mass flow fluctuations resulting from acoustic effects in the suction and discharge manifolds. Through proper geometric design of the manifolds, these pulsations can be modified to increase efficiency and reduce noise. This paper documents the development of a computer simulation program used to tune rolling piston vapor compressors. The FORTRAN program models the mechanical, fluid, thermodynamic, kinematic, and acoustical processes occurring in such compressors. Suction and discharge chamber pressures, mass flow rates, valve displacements, and acoustic input and transfer impedances are expressed in numerical and graphical form. Experimental acoustic pressure measurements from a refrigerator test stand provide validation.

INTRODUCTION

The development of rolling piston vapor compressors (Figure 1) represents one response by the major appliance industry to the need for efficient, quiet, and low cost refrigeration systems. Suction and discharge processes in such machines are periodic and unsteady; thus, they give rise to mass flow and pressure fluctuations in the manifold systems. These pulsations consist of acoustic plane waves that affect both noise levels and efficiency by modifying the refrigerant flow rates. The magnitude and frequency of these waves are in turn influenced by the manifold system geometries. Experimental tuning studies are very expensive and time consuming. Consequently, a computer simulation program that modeled the phenomenon while predicting design sensitivities and performance parameters would be a powerful design tool.

Objectives and Scope

This paper documents the development and structure of a simulation program, PSIMP (Polytropic Model Simulation Program), that models the mechanical, thermodynamic, fluid, kinematic, and acoustical processes occurring in rolling piston vapor compressors. As the program name implies, a polytropic model is used to simulate the compression and expansion processes. Acoustic modeling routines determine the input and transfer function impedance and phase. Additional routines model the flow processes, valve dynamics, and kinematic behavior of the system. The routines are used in a numerical procedure that computes chamber pressure, mass flow, and valve displacement as a function of eccentric crank angle. Iteration continues until mass flow and discharge valve pressures converge to values from the previous iteration. Simulation results are written to a formatted output file and graphically displayed.

The program is written in FORTRAN and designed to run on a VAX system equipped with Tektronix graphics terminals. Plotting routines use a combination of PLOT10 Terminal Control System (TCS) commands, and Interactive Graphics Library (IGL) functions to graphically display the simulation results. English units are used for the calculations; however, with minor alterations, the program could be adapted for use with SI units. The simulation package is validated by comparing program results with analytical solutions and experimental data.

Review of Previous Work

Existing literature on vapor compressors is quite extensive, but most computer simulation work has been limited to reciprocating machines [1-3]. Acoustic effects were incorporated into single cylinder and multiple cylinder models through work performed by Soedel and Singh [4-7]. Nieter, along with Singh, developed a comprehensive simulation program using acoustic transfer matrices to model multiple cylinder reciprocating machines and conduct parametric tuning studies [8]. Prater, et al., investigated the effects of condenser impedance characteristics on mass flow rates, cylinder pressure profiles, and compressor performance parameters [9].

The literature on rolling piston type vapor compressors is much more limited, and most of the available studies address specific mechanical design issues. Examples include investigations of kinematics and kinetics, starting characteristics, tribology, bearing quality, vane slot clearance, valve design, and fluid leakage [10-17].

THEORY

The simulation program requires mathematical models for the cylinder kinematics and thermodynamics, valve dynamics, fluid flow through the valve, acoustic characteristics of the manifold, and interaction between the cylinder and manifolds. Program assumptions include

- Polytropic equation of state for the compression and charging processes
- Ideal gas working fluid
- One-dimensional fluid flow
- Constant crankshaft angular velocity
- Suction chamber fluid state is the same as the fluid at the suction port
- Damped, single degree of freedom valve displacement model
- Unsteady, isentropic flow through the valve
- Acoustic plane wave theory is valid

Fluid leakage, cylinder heat transfer, lubrication effects, variable rolling piston velocity, friction, and motor dynamics are not directly modeled.

Kinematic Model

The kinematic model represents chamber volume as a function of the crank angle, θ. Upon assuming constant crankshaft velocity, ω, the steady state compression chamber volume is given by [12]

$$V(\theta) = V_t - \tfrac{1}{2}R^2\ell\theta + \tfrac{1}{2}r^2\ell(\theta+\alpha) + \tfrac{1}{2}e\ell(r+r_v)\sin(\theta+\alpha) - \tfrac{1}{2}r_v^2\ell\tan\alpha - \tfrac{1}{2}b\ell x\,, \qquad (1a)$$

$$V_t = \pi(R^2-r^2)\ell, \qquad \alpha = \sin^{-1}\left[\frac{e}{(r+r_v)}\sin\theta\right], \qquad x = R+r_v-(r+r_v)\cos\alpha - e\cos\theta. \qquad (1b,c)$$

V_t = total volume
b = cylinder height
x = vane extension
R = cylinder radius
ℓ = cylinder height
r_v = vane tip radius
r = roller radius
e = relative eccentricity, R-r

The mean volumetric flow rate then becomes

$$\frac{dV}{dt} = \tfrac{1}{2}\omega\ell(r-R) + \tfrac{1}{2}r^2\ell\,\frac{d\alpha}{dt} + \tfrac{1}{2}e\ell(r+r_v)\left(\omega+\frac{d\alpha}{dt}\right)\cos(\alpha+\theta) - \tfrac{1}{2}r_v^2\ell\sec^2\alpha\,\frac{d\alpha}{dt} + \tfrac{1}{2}b\ell\frac{dx}{dt}, \qquad (2a)$$

$$\frac{dx}{dt} = (r+r_v)\sin\alpha + e\omega\sin\theta, \qquad \frac{d\alpha}{dt} = \frac{e\omega\cos\theta}{r+r_v}\left[1-\left(\frac{e}{r+r_v}\sin\theta\right)\right]^{-\frac{1}{2}}. \qquad (2b,c)$$

Using the volume velocity determined with Eq. 2 and the fluid equation of state, the suction gas density and mass flow can be evaluated at each crank angle increment.

Thermodynamic Modeling

The working fluid in the simulation program is assumed to behave as an ideal gas, $p_c v_c = R_g T_c$, where p_c, v_c, and T_c are the chamber pressure, specific volume, and temperature, respectively, and R_g is the universal gas constant. When this expression is combined with a polytropic process model, $p_c v_c^n = \text{constant}$, the state of the refrigerant in the compression chamber can be fixed using the following relations:

$$p_c(\theta)=\left(\frac{m_c(\theta)}{\rho_o V_c(\theta)}\right)^n, \qquad T_c(\theta)=T_o\left(\frac{p_c(\theta)}{p_o}\right)^{\frac{n-1}{n}}. \tag{3a,b}$$

Here n is the polytropic constant, m_c is the total cylinder mass, and ρ_o, T_o, and p_o are the chamber density, temperature, and pressure at the beginning of the cycle. While the ideal gas model applies to both the intake and discharge process, the lack of a valve means that the refrigerant state for the suction chamber is fixed by the line conditions and port location.

Valve Dynamics

The dynamic behavior of the discharge valve has a major influence on flow pulsation levels. To include inertia, energy dissipation, and stiffness effects, the valve is modeled as a linear, single degree of freedom mass-spring-damper system. Also included in the model are the valve preload, F_o, and the valve stop height. The differential equation of motion for the system then becomes

$$\frac{d^2y_v(t)}{dt^2}+2\zeta_v\omega_n\frac{dy_v(t)}{dt}+\omega_n^2y_v(t)=\frac{F_p(t)-F_o}{m_v}, \tag{4a}$$

$$F_p(t)=[p_c(t)-p_d(t)]A_v(t), \qquad \omega_n=\sqrt{\frac{k_v}{m_v}}, \qquad \zeta_v=\frac{c_v}{2m_v\omega_n}. \tag{4b-d}$$

y_v = valve displacement
m_v = effective valve mass
k_v = effective valve stiffness
c_v = viscous damping coefficient
ω_n = undamped natural frequency
ζ_v = valve damping ratio
p_c = compression chamber pressure
p_d = manifold pressure at valve
F_p = net pressure force
A_v = valve force area

The valve pressure force is determined from the pressure differential and force area [1]. Valve force area, A_v, can be assumed to be equivalent to the port area, computed analytically or determined experimentally. Although actual compressor reed valves are multiple degree of freedom systems with a large number of natural frequencies, this simplified model is sufficient because the largest cylinder pressure harmonics do not strongly excite higher modes.

Valve Flow Model

Discharge flow areas at discrete valve displacements are entered into the program from an input data file. These values should be determined by the user, preferably by experiment. The discharge process is then modeled as unsteady, isentropic, ideal gas flow through an orifice [7]:

$$\dot{m}_v=C_d(\theta)A_f(\theta)p_u(\theta)\sqrt{\frac{2g_c}{(k-1)R_gT_u(\theta)}\left[r_p(\theta)^{\frac{2}{k}}-r_p(\theta)^{\frac{k+1}{k}}\right]}, \tag{5}$$

$$r_p=\frac{p_v}{p_u}\ (r_p>r_c), \qquad r_p=r_c\ (r_p\le r_c), \qquad r_c=\left(\frac{2}{k+1}\right)^{\frac{k}{k-1}} \tag{6a-c}$$

$\dot{m}_v$ = valve mass flow rate
A_f = valve flow area
C_d = valve discharge coefficient
k = specific heat ratio
T_u = upstream fluid temperature
r_c = pressure ratio for choked flow
p_u = upstream pressure
p_v = downstream pressure

Note that the "upstream" and "downstream" notations refer to the flow direction. Because no significant flow restrictions exist in the suction line, the nominal mass flow rate through the suction port is determined kinematically, using Eq. 2.

Acoustic Manifold Modeling

The compressor manifolds are modeled by discretizing the systems into subsystems whose dynamic behavior can be analytically described with four pole transfer matrices. In this scheme linear acoustic elements are represented in terms of input and output variables representing acoustic volumetric flow rate and acoustic pressure. An assumption of one-dimensional plane wave propagation limits the upper analysis frequency to

$$f_{max} = \frac{c}{2D_{max}} \text{ (Hz)}, \qquad c = \sqrt{kR_g T}, \tag{7a,b}$$

where D_{max} is the hydraulic diameter of the largest element in the manifold. The sonic velocity in the gas medium, c, is defined by Eq. 7b.

An acoustic element usually represents a discontinuity in the manifold system. These discontinuities are assumed to be abrupt to eliminate acoustic diffraction [7,18]. The model is built by connecting elements in series and parallel. A passage that has multiple section changes requires the use of several elements of appropriate size and type. Six element types are utilized: (i) constant cross section tube, (ii) lumped volume cavity, (iii) identity connection, (iv) anechoic termination, (v) open termination, and (vi) closed termination.

The most commonly used element is the constant cross section tube. Passages of this type are common in compressor manifolds, and their acoustic behavior is well understood from analytical and experimental studies. Both inertia and compliance effects are present in the analytical model, and energy dissipation can be taken into account through the use of an empirical damping factor [7,19]. Large cavities that appear in the system can be represented as lumped volumes. Unlike the constant cross section tubes, these elements model only fluid compliance effects. The identity connection allows specification of an output position, but does not affect the system dynamics or simulation results. The anechoic termination element represents an infinitely long duct in which acoustic waves propagate without reflection. An open tube with zero acoustic pressure at its boundary is modeled with an open termination element, while a closed termination simulates a rigid boundary with infinite impedance and zero volume velocity. The theory supporting the application of these models is well developed in the open literature [6,7,20].

Coupling of the linear acoustic elements occurs in the frequency domain, and is based on two port network theory [21]. In the acoustic variant of this approach, we express the relationship between input and output variables for the i-th element in a manifold system as

$$\begin{aligned} p_{in}(\omega) &= A(\omega)p_{out}(\omega) + B(\omega)q_{out}(\omega) \\ q_{in}(\omega) &= C(\omega)p_{out}(\omega) + D(\omega)q_{out}(\omega) \end{aligned}, \tag{8a,b}$$

or in matrix form as

$$\begin{Bmatrix} p(\omega) \\ q(\omega) \end{Bmatrix}_{in} = [\Delta]_i \begin{Bmatrix} p(\omega) \\ q(\omega) \end{Bmatrix}_{out}, \qquad [\Delta]_i = \begin{bmatrix} A_i(\omega) & B_i(\omega) \\ C_i(\omega) & D_i(\omega) \end{bmatrix}. \tag{9a,b}$$

Here the acoustic pressure, p, serves as the across variable, and the acoustic volume velocity, q serves as the through variable.. The transmission matrix, [Δ], is sometimes referred to as a four pole matrix. Four pole parameters A, B, C, and D depend on the element geometry and oscillation frequency, and like the acoustic variables, are generally complex valued.

Coupling techniques for series and branch connected transfer matrices are well documented in the open literature, and so are omitted here. The result of the operation is a complex valued, frequency domain description of the dynamic relationship between acoustic input and output variables. Equations 8 can be solved simultaneously for the acoustic pressures in terms of the volume velocities:

$$\begin{Bmatrix} p_{in}(\omega) \\ p_{out}(\omega) \end{Bmatrix} = \begin{bmatrix} z_{11} & z_{12} \\ z_{21} & z_{22} \end{bmatrix} \begin{Bmatrix} q_{in}(\omega) \\ q_{out}(\omega) \end{Bmatrix}, \quad z_i = z_{11} = \frac{p_{in}}{q_{in}}(\omega) = \frac{A(\omega)}{C(\omega)} \text{ (acoustic input impedance)}, \tag{10,11}$$

$$z_T = z_{12} = z_{21} = \frac{p_{in}}{q_{out}}(\omega) = \frac{1}{C(\omega)} \quad \text{(acoustic transfer impedance)} \tag{12}$$

Note that the output impedance, z_{22}, is rarely of interest. A transfer function that does find use in a simulation program of this type is the acoustic pressure ratio. This quantity is given by

$$\frac{p_{out}}{p_{in}}(\omega) = \left(\frac{p_{out}}{q_{in}}\right)\left(\frac{q_{in}}{p_{in}}\right) = \frac{z_{21}}{z_{11}} = \frac{1}{A(\omega)}. \tag{13}$$

The transfer functions of Eqs. 11-13 thus represent a frequency domain description of the manifold. If an impedance or pressure ratio at an intermediate point within the manifold system is required, the element cascading procedure is somewhat different.

Coupling Compressor and Manifold Models

The complete simulation program is structured to include the acoustic effects of manifold systems on the physical processes that occur in the compressor body during the compression and expansion of the refrigerant. For the purpose of simplifying the computational routines, the compressor simulation is performed in the time domain while the acoustic effects are determined in the frequency domain. The two computations are related by the mass flow rate and fluid state. The compressor simulation routines yield chamber pressure and mass flow as a function of the crank angle ($\theta = \omega t$). As an example, consider a discharge process yielding an initial mass flow rate profile consisting of i=1,2,...,M discrete values. We begin by expressing the profile as a finite Fourier expansion expressed in terms of the crank angle:

$$\dot{m}_v(\theta_i) = \frac{M_0}{2} + \sum_{n=1}^{N} M_n \cos(n\theta_i - \psi_n), \qquad M_n = \sqrt{a_n^2 + b_n^2}, \qquad \tan(-\psi_n) = \frac{b_n}{a_n}, \tag{14a-c}$$

$$a_v(n\omega) = \frac{\delta}{\pi} + \sum_{i=0}^{M} \dot{m}_v(\theta_i)\cos(n\theta_i), \qquad b_v(n\omega) = \frac{\delta}{\pi} + \sum_{i=0}^{M} \dot{m}_v(\theta_i)\sin(n\theta_i), \tag{14d,e}$$

M_n = mass flow harmonic magnitude
ψ_n = mass flow harmonic phase
δ = crank increment
N = number of crank harmonics
a_v = discrete Fourier cosine coefficient
b_v = Discrete Fourier sine coefficient
n = crank speed harmonic index

Volume velocities are obtained by dividing the result of Eq. 14b by the average fluid density. The corresponding fluid states from the time domain are used to calculate the sonic velocity in the valve chamber and suction line. These values are used to develop the four pole matrices containing the input and transfer impedance values. The product of the volume velocity and transfer or input impedance then yields the frequency domain acoustic manifold pressures at the discharge valve (p_1) and a second, user specified manifold location (p_2):

$$p_1(n\omega) = z_1(n\omega)Q_1(\omega), \qquad p_2(n\omega) = z_T(n\omega)Q_1(\omega). \tag{15a,b}$$

An inverse Fourier transform then reconstructs the acoustic pressures in the time domain, and the new profiles can then be used to correct mass flow rates during the next iteration.

PROGRAM STRUCTURE

A flowchart showing the structure of PSIMP is shown in Figure 2. The program is initiated by an input data file consisting of compressor geometric information, fluid properties, valve characteristics, and element parameters for the manifold systems. The discharge valve force area can be assumed equal to the port area, or entered as a table of data with the area tabulated at discrete valve displacements. Discharge flow area is entered in a similar fashion. Valve parameters are entered in the form of the static stiffness, fundamental frequency, equivalent viscous damping ratio, and valve stop height.

Several preliminary calculations are made to initialize the main simulation loop. These include determining the pressure ratio for choked flow, initial refrigerant density, pressure and impedance reference values, and effective mass of the discharge valve. The main iteration loop simulates one cycle of crank motion. The suction and discharge parameters are computed simultaneously, with the final suction state becoming the initial discharge state for subsequent iterations. The loop is repeated until mass flow and manifold pressure profiles converge to within a specified criterion.

The most important part of the simulation is the interaction between the chamber pressures and manifold pressures. These processes are rather straight forward on the discharge side. The valve equation of motion, compression chamber equation of state, and fluid flow equation are all solved simultaneously using a fourth-order Runge-Kutta technique. For the first iteration, the discharge pressure is assumed constant and the initial mass is specified by the maximum discharge chamber volume and mean suction pressure. A discrete Fourier transform is applied to the computed mass flow rate, and these values are used with the discharge acoustic input impedance to compute a corrected line pressure profile. The new pressures then provide more exact mass flow values during the next iteration, which in turn lead to an even more accurate pressure profile. At the start of each discharge iteration beyond the initial loop, mass balance and pressure results from the suction simulation provide increasingly accurate initial values.

The suction simulation is quite different. The lack of a port valve means that pulsations in the suction line have a direct and immediate effect on the mass flow rate. The suction volume velocity (volumetric flow rate) is fixed by the crank speed and kinematic differential volume relation. This value is used with the suction manifold input impedance to determine an initial approximation for the suction line acoustic pressures, which are then used with the equation of state to compute a corrected mass flow profile. The entire process is repeated concurrently with the discharge chamber iterations until convergence is achieved.

Post-processing routines conclude the simulation by calculating cyclic performance parameters such as volumetric efficiency, performance index, work per cycle, power and torque required, mean and extreme pressure values, and net mass flow per cycle. In particular, the total work per cycle is given as

$$W_{cycle} = \int_{cycle} pdV \tag{16}$$

Suction underwork and discharge overwork are calculated in a similar fashion, with the pressure term in Eq. 20 being replaced by the difference between the chamber pressure and average acoustic pressure at the port.

PRESENTATION OF RESULTS

Results are presented in both tabular and graphical form. Tabular output echoes the input data, lists the performance parameters, and displays volume, temperature, chamber and line pressure, fluid mass, mass flow rate, and valve displacement as a function of the crank angle. Frequency domain results consist of impedance transfer function values, as well as pressure and mass flow rate harmonic data. The graphical displays include:

1. Suction/Discharge Chamber Pressure Versus Crank Angle The chamber pressure profile experienced by a single control mass is plotted, rather than that of the two distinct control volumes that exist during each crank revolution. Consequently, the ordinate crank angles measured relative to the roller/vane contact position extend from 0° as the suction volume increases from zero, through 360°, where the suction volume becomes the compression volume, to 720° as the compression volume approaches zero.

2. Suction Port and Discharge Line Pressure Versus Crank Angle This plot explicitly shows the manifold pressure pulsations present in the compressor. An experienced analyst will be able to interpret the phasing of the pulsation and determine whether they help or hinder the flow processes.

3. Discharge Valve Displacement Versus Crank Angle These curves are useful in the design of the valve reed and stop. They are also displayed with the chamber and line pressures. The time domain pressure and valve displacement curve are displayed simultaneously.

4. Instantaneous Mass Flow Rates Versus Crank Angle These plots allow any back flow through the suction or discharge ports to be identified, and also play a major part in the tuning process by helping maximize capacity.

5. Chamber Pressure Versus Chamber Volume A standard p-V diagram depicts the thermodynamic cycle over two crank rotations.

6. Manifold Impedance Transfer Functions These values are computed and displayed as a function of crank speed harmonic. Large magnitudes can indicate the presence of a low frequency resonance condition that might greatly affect mass flow rates, or a higher frequency resonance that might create objectionable noise.

7. Pressure and Flow Rate Spectra This frequency domain information complements the time domain displays of these profiles. Used with the manifold system transfer functions, it helps a designer tune the manifold geometry so that only desirable resonance peaks are excited.

Figure 3 presents sample results from a fictitious, but realistic model file. Note in particular the significant magnitude of the discharge line pulsations (Figure 3a, 8-9 psia). Suction line pulsations are so low (.9-1.0 psia) that they are unnoticeable on the chosen scale. The discrepancy is due to the lack of a suction valve. Figure 3b shows that the suction flow rate profile has a longer duration, smaller maximum value, and smoother shape than the discharge profile. This translates into lower volume velocity magnitudes at the crank speed harmonics, and less excitation for suction manifold acoustic modes.

EXPERIMENTAL VALIDATION

Experimental validation of the program results was performed by measuring acoustic manifold pressures on a rolling piston compressor mounted in a refrigerator test stand. Piezoelectric pressure transducers were used, while data acquisition and signal processing tasks were performed by a Macintosh based system built around LabView, a software package that digitally simulates laboratory instruments. In our application we used the package as a combination digital oscilloscope and two channel FFT analyzer.

Data from different points along the suction and discharge systems match the simulation results quite well. Figure 4a shows time and frequency domain acoustic pressures measured in the discharge line just outside the shell. Figure 4b shows PSIMP predictions at the same point. Although pulsation amplitude was quite small (about 0.4 psia peak-to-peak), the analytical and experimental results agree closely in amplitude, frequency content, and phasing. Note that the small amplitudes are due to the measurement point, which was well downstream from muffling elements. As noted, the program predicts much larger pressure amplitudes near the discharge valve.

CONCLUDING REMARKS

PSIMP is now being used as an optimization tool to investigate design changes for an actual compressor used in household refrigerators. The program can be improved by developing more accurate models for the compressor components and processes that influence steady state operation. These models include variable crank shaft velocity, multiple degree of freedom valve behavior, fluid leakage, and nonlinear effects due to mean fluid flow. It should also be possible to better fix the mean refrigerant states through an energy balance based upon the first law of thermodynamics. The manifold modeling process can be improved by defining new acoustic elements that make use of experimental impedance measurements and acoustic finite element results. Many of these modifications are currently being implemented.

REFERENCES

[1] Soedel, W., "Introduction to Computer Simulation of Positive Displacement Type Compressors," Purdue University, 1974.

[2] Hamilton, J.F., "Extensions of Mathematical Modeling of Positive Displacement Type Compressors," Purdue University, 1972.

[3] Prater, G., Nieter, J., and Singh, R., "Simulation of Cylinder Pressure Overloading Caused by the Slugging Conditions, Volume 1." Research report submitted to the Copeland Corporation, 1984.

[4] Singh, R., "Modeling of Multicylinder Compressor Discharge Systems," Ph.D. Thesis, Purdue University, 1975.

[5] Soedel, W., "Gas Pulsations in Compressor and Engine Manifolds," Ray W. Herrick Laboratories Report, Purdue University, 1978.

[6] Singh, R. and Soedel, W., "Assessment of Fluid-Induced Damping in Refrigeration Machinery Manifolds," Journal of Sound and Vibration, 1978, Vol. 57, pp. 449-452.

[7] Singh, R. and Soedel, W., "Mathematical Modeling of Multicylinder Compressor Discharge System Interactions," Journal of Sound and Vibration, 1979, Vol. 63, pp. 125-143.

[8] Nieter, J., "A Computer Simulation and Modal Analysis Study of Compressor Manifolds and Tuning Phenomena," M.Sc. Thesis, The Ohio State University, 1983.

[9] Prater, G., Farstad, J., and Singh, R., "Compressor Pulsations and System Interaction." Research report submitted to the Copeland Corporation, 1985.

[10] Okada, K. and Kuyama, K., "Motion of Rolling Piston in Rotary Compressor," Purdue Compressor Technology Conference, 1982.

[11] Sakurai, E. and Hamilton, J.F., "Measurement of Operating Conditions of Rolling Piston Type Rotary Compressors," Purdue Compressor Technology Conference, 1982.

[12] Yanagisawa, T. and Shimizu, T., "Motion Analysis of Rolling Piston in Rotary Compressor," Purdue Compressor Technology Conference, 1982.

[13] Ishii, N., Imaichi, K., and Muramatsu, S., "The Study of Rolling Piston, Rotary Compressor Dynamic Behavior When Stopping to Reduce Noise and Vibration Level," International Compressor Engineering Conference at Purdue, 1984.

[14] Jorgensen, S.H. and Nissen, H.S., "Mechanical Loss Model of Rolling Piston Rotary Compressor With Special Importance Attached to Journal Bearing," International Compressor Engineering Conference at Purdue, 1984.

[15] Itami, T., Kubo, M., and Sugiyama, M., "Estimation of Bearing Load of Rolling Piston Type Rotary Compressors Under High Speed Operation," International Compressor Conference at Purdue, 1986.

[16] Okoma, K. and Onoda, I., "Study of Lubrication Mechanism for Horizontal Type Rolling Piston Rotary Compressor," International Compressor Engineering Conference at Purdue, 1988.

[17] Yanagisawa, T., Shimizu, T., and Horioka, T., "A Study on Starting Characteristics of a Rolling Piston Type Rotary Compressor," International Compressor Engineering Conference at Purdue, 1988.

[18] Rschevkin, S.N., A Course of Lectures on the Theory of Sound, McMillian Co., New York, 1963.

[19] Kammin, H., "The Development and Experimental Verification of an Acoustic Damping Model for a Frequency Domain Digital Pulsation Simulation," International Compressor Engineering Conference at Purdue, 1988.

[20] Kim, J. and Soedel, W., "Four Pole Parameters of Shell Cavity and Application to Gas Pulsation Modeling," International Compressor Engineering Conference at Purdue, 1988.

[21] Harman, W.W. and Lytle, D.W., Electrical and Mechanical Networks, McGraw-Hill, New York, 1962.

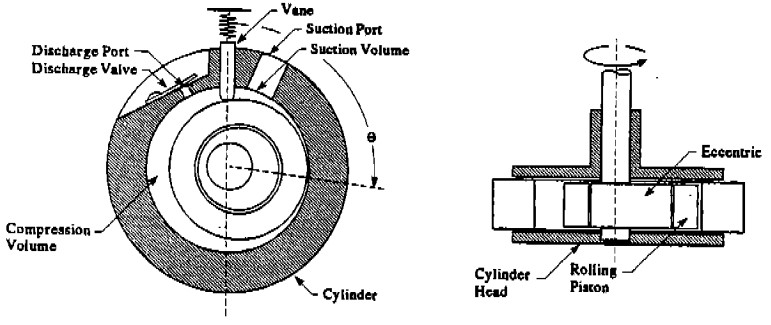

Figure 1. Mechanical components of a rolling piston vapor compressor.

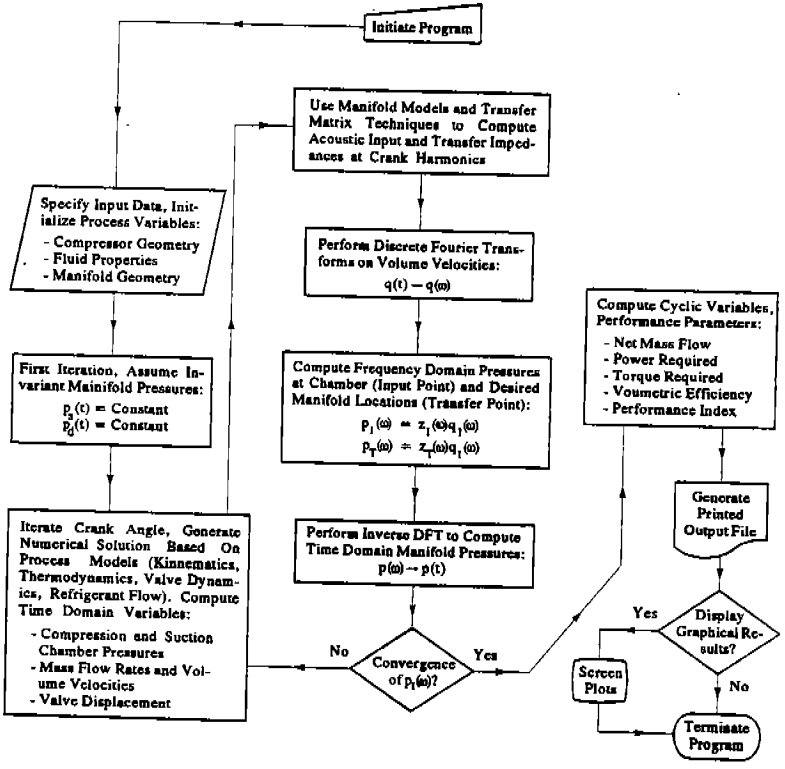

Figure 2. Logic structure, Polytropic Model Simulation Program.

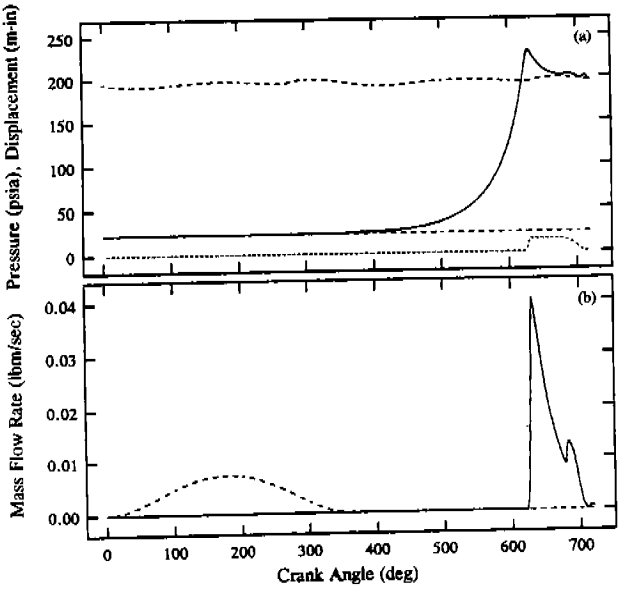

Figure 3. Representative results from PSIMP. (a) Chamber pressure (———), discharge and suction line pressures (-------), and discharge valve displacement (·····) versus crank angle. (b) Discharge (———) and suction (-------) mass flow rate versus crank angle.

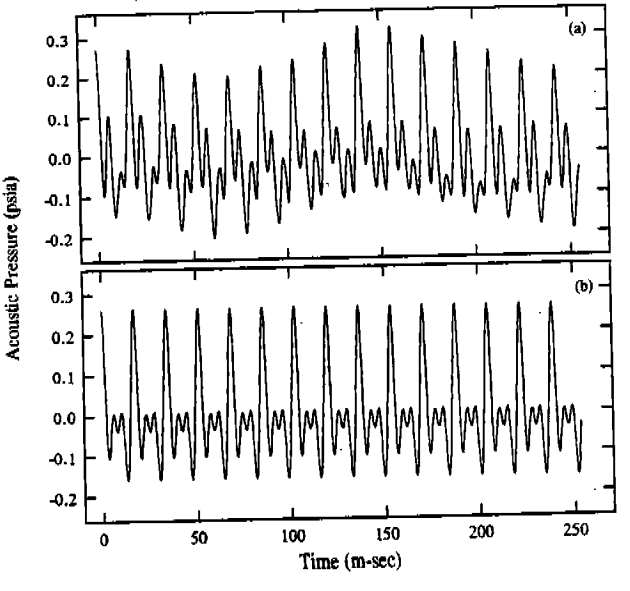

Figure 4. Comparison of experimental and analytical pulsation results. (a) Time domain discharge line pressure measured near shell exit . (b) Corresponding prediction from PSIMP.